European Journal of Chemistry 1 (4) (2010) 381-384

European Journal of Chemistry

Journal homepage: www.eurjchem.com

Analytic perturbation theory to study the effect of screening on alignment of atomic inner shell vacancies

Ajay Sharma[a,*] and Raj Mittal[b]

[a] *Physics Department, Chitkara University, Solan, Himachal Pradesh, IN-174103, India*
[b] *Physics Department, Nuclear Science Laboratories, Punjabi University, Patiala, IN-147002, India*

**Corresponding author at: Physics Department, Chitkara University, Solan, Himachal Pradesh, IN-174103, India. Tel.: +91.172.4691800; fax: +91.172.4691800.*
E-mail address: ajayph75@gmail.com (A. Sharma).

COMMUNICATION INFORMATION

Received: 22 May 2010
Received in revised form: 08 August 2010
Accepted: 08 August 2010
Online: 31 December 2010

KEYWORDS

Perturbation theory
Screening effect
Vacancy alignment
Non-relativistic dipole approximation
L sub-shells

ABSTRACT

An analytic perturbation theory has been developed for screened Coulomb radial wave functions by interpolating the screened Coulomb potential of McEnnan for elements lanthanum to uranium and was used to calculate alignment of vacancies in L3 sub shell. To check the authenticity of the present method of calculation, the intermediate steps are compared with our earlier formulation of point Coulomb potential for the calculations. A close agreement has been obtained among the values of intermediate steps involved in both the formulations that proved the reliability of present calculations and prompted us to extend the calculations for the elements lanthanum to uranium in the energy region threshold to 60 keV.

1. Introduction

For photon induced atomic processes, Flügge *et al.* [1] were the first to explore the alignment of atomic inner shell vacancies. Calculations of vacancy alignment with different approaches have been performed by different workers, but some systematic numerical calculations were provided by Berezhko *et al.* [2] and Kleiman and Lohmann [3]. Up to date, the survey of literature reveals that, since eighties, the experimental measurements on alignment of photon induced L3 vacancies from anisotropic distribution of fluorescent X-rays in some rare earth and high Z elements are available from the work of eight different groups [4] those predicted contradictory results. To check the discrepancies of the results from different experimental groups and the results from experiment and theory as pointed out above, the effect of electron screening potential on the alignment calculations are undertaken in the present paper. Our earlier theoretical calculations [5] are treated as reference to observe the impact of screening on the alignment and are refined by applying screening correction [6]. In addition, an analytic perturbation theory has been developed for screened Coulomb radial wave function by interpolating the screened Coulomb potential of McEnnan *et al.* [7] for the elements La to U in the energy region threshold to 60 keV.

2. Formulation

The L shell electrons being next to those in K shell are likely to be under screened potential. Therefore, each L electron seems to move in a screened Coulomb field, $(Z–s).e/r^2$ of the nucleus that modifies the earlier considered potential energy. L3 vacancy alignment is accounted in term of alignment parameter A_2 that is fractional difference in ionization cross-sections of L3 magnetic sub-states. The present Z region for which A_2 has been generated is prone to screening and two different attempts have been made to study the effect of screening by;

(i) Accommodating effect of screened Coulomb potential on the earlier generated alignment parameter A_2 data [5] and
(ii) Developing an analytic perturbation theory [7] for screened Coulomb wave functions in a non-relativistic dipole approximation which, in turn, is used for the calculation of A_2 for photon induced L3 vacancies in high Z elements, $57 \leq Z \leq 92$.

3. Effect of screened Coulomb potential

To treat the L shell electrons under the screening nuclear pull, a screened Coulomb potential, (Z–s)e/r, of the nucleus is considered [8] instead of Ze/r in the case of ordinary point Coulomb potential where s is the screening constant. Slater [6] has suggested the rules in order to decide the value of the screening constant s and for a 2s or 2p electron, s value comes as;

$$s = 2(0.85) + 7(0.35) = 4.15 \quad (1)$$

Therefore, in a screened Coulomb potential the value $a = Z\alpha$ is to be modified as, $a^* = (Z - s)\alpha$, where α is fine structure constant. The modified value a^* affects equations of formulation [5], which in turn modified single particle radial integrals R_2^* for the bound (L=1) and continuum ($\ell' = 2$) states and R_0^* for bound (L=1) and continuum ($\ell' = 0$) as;

ISSN 2153-2249 (Print) / ISSN 2153-2257 (Online)
DOI:10.5155/eurjchem.1.4.381-384.121

$$R_2^* = 0.0068(a^{*5/2})p^2[\exp(1.57(a^*/p))]\left|\Gamma(3+i(a^*/p))\right|\times \quad (2)$$
$$\int_0^\infty \{r^6[\exp(ip-a^*/2)r]_1F_1\left[3-i\left(\frac{a^*}{p}\right),6;(-2ipr)\right]\}dr$$

$$R_0^* = 0.2041a^{*5/2}p^2[\exp(1.57a^*/p)]\left|\Gamma(1+i(a^*/p))\right|\times \quad (3)$$
$$\int_0^\infty \{r^4[\exp(ip-a^*/2)r]_1F_1\left[3-i\left(\frac{a^*}{p}\right),6;(-2ipr)\right]\}dr$$

Thus, for $2p_{3/2}$ state, the modified alignment parameter (A_2^*) under screened Coulomb potential is

$$A_2^* = \frac{\left|R_0^*\right|^2 + \frac{1}{5}\left|R_2^*\right|^2}{2\left|R_0^*\right|^2 + 4\left|R_2^*\right|^2} \quad (4)$$

In this paper, the screened alignment parameter A_2^* has been calculated for the elements $57 \le Z \le 92$ at incident photon energy varying from L3 threshold to 60 keV. The calculated results are illustrated in Figure 1-5.

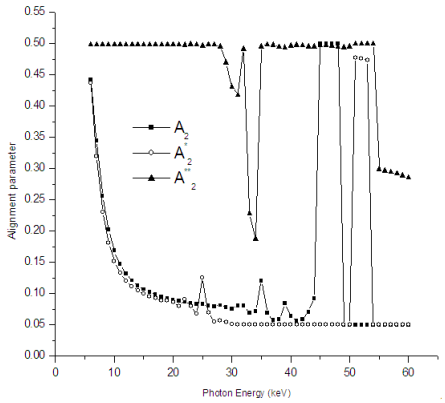

Figure 1. Plots of alignment parameter (A_2) without screening and (A_2^*, A_2^{**}) with screening at photon energies threshold to 60 keV for La.

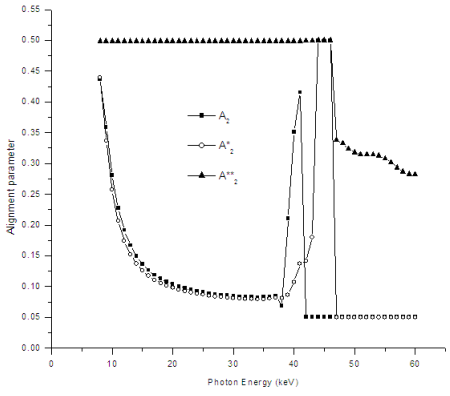

Figure 2. Plots of alignment parameter (A_2) without screening and (A_2^*, A_2^{**}) with screening at photon energies threshold to 60 keV for Gd.

4. Analytic perturbation theory for screening effect

For a non-relativistic radial wave function in a screened Coulomb potential, the potential inside an atom, according to analytic perturbation theory, is [7]

$$V(r) = \left(\frac{a}{r}\right)\left[1 + V_1(\lambda r) + V_2(\lambda r)^2 + V_3(\lambda r)^3 + \ldots\ldots\right] \quad (5)$$

Here $a = Z\alpha$ and $\lambda = \alpha Z^{1/3}$ characterize the screening. Coefficients V_k's are of the order of unity. V_k's are alternate in sign and decrease with increasing k and the equation (4) converge in the region $\lambda r<1$.

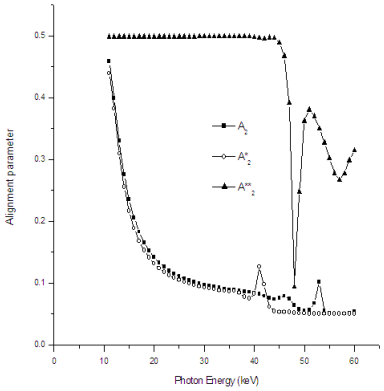

Figure 3. Plots of alignment parameter (A_2) without screening and (A_2^*, A_2^{**}) with screening at photon energies threshold to 60 keV for W.

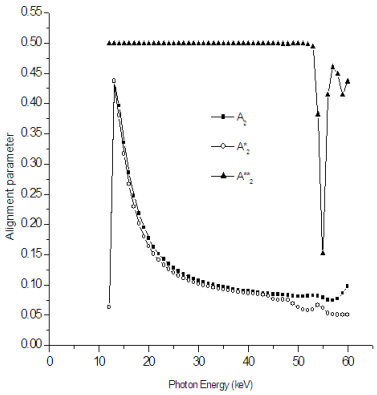

Figure 4. Plots of alignment parameter (A_2) without screening and (A_2^*, A_2^{**}) with screening at photon energies threshold to 60 keV for Au.

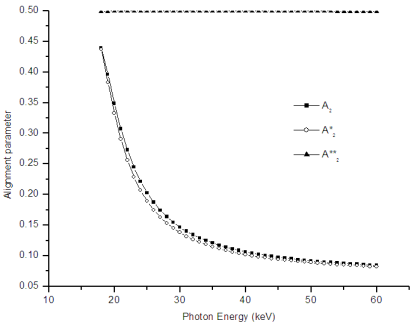

Figure 5. Plots of alignment parameter (A_2) without screening and (A_2^*, A_2^{**}) with screening at photon energies threshold to 60 keV for Th.

In non-relativistic dipole approximation for this type of potential, the formulation [5] changes as under;

(i) Bound state wave function $\Re_{n\ell}(r)$ is modified as

$$\Re^{**}{}_{n\ell}(r) = N_{n\ell}{}^{**} r^\ell e^{-ar/2} S^{**}{}_{n\ell}(r) \quad (6)$$

The term $S^{**}{}_{n\ell}(r)$ replaces the confluent hypergeometric function used in the previous formulation [5]. Here $N^{**}{}_{n\ell}$ is the modified normalization constant and for the bound state and for 2p state (for ℓ=1), it becomes

$$N^{**}_{21} = N_{21}(1-30\Lambda_2-320\Lambda_3) \quad (7)$$

where $N_{21}=\frac{(a)^{5/2}}{6}\left(\frac{3}{2}\right)^{1/2}$ is the point Coulomb normalization for the 2p state and

$$\Lambda_k = V_k(\lambda/a)^k \equiv V_k(1.13Z^{-2/3})^k \quad (8)$$

The values of V_k's, for k=2 and 3 and for the elements Z=57 to 92, are obtained by interpolating [9] the screened Coulomb potentials of McEnnan *et al.* [7].

The radial wave function $S_{n\ell}^{**}(r)$ is a polynomial in r and, for 2p state, it becomes

$$S^{**}_{21}(r) = 1+\Lambda_2(ar)^2+2\Lambda_3(ar)^2(3+\frac{1}{3}ar) \quad (9)$$

Thus, the final form of the bound state wave function for n=2 and ℓ=1 is

$$\Re^{**}_{21}(r)=\frac{a^{5/2}}{6}\left(\frac{3}{2}\right)^{1/2}\left[1-30\Lambda_2-320\Lambda_3\right]re^{-ar/2} \left\{1+\Lambda_2(ar)^2+2\Lambda_3(ar)^2(3+\frac{1}{3}ar)\right\} \quad (10)$$

Screening also affects the binding energy of the L3 electron and the modified binding energy becomes [10]

$$BE^{**} = -\frac{1}{8}a^2\left(1+8\Lambda_1+40\Lambda_2+240\Lambda_3\right) \quad (11)$$

(ii) The continuum states $\ell'=\ell\pm1$ i. e. (ℓ' = 2 and 0), the modified radial wave function is

$$\Re^{**}_{p'\ell'} = N^{**}_{p'\ell'}r^{\ell'}e^{-ipr}S^{**}_{\ell'}(pr) \quad (12)$$

where p' is the magnitude of the asymptotic momentum for screened wave function [9];

$$p' = p+\Delta p \quad \text{and} \quad \Delta p = \sqrt{\frac{2(BE^{**}-BE)}{511}} \quad (13)$$

$$N^{**}_{p'\ell'} = N_{p'\ell'}\frac{p^{1/2}}{(2\pi)^{3/2}}\begin{bmatrix} 1+\frac{1}{4}\Lambda_2\nu^2\left\{\begin{matrix}\ell'(\ell'+1)(2\ell'+1)-[3\nu^2+\ell'(\ell'+1)+3n^2-\ell(\ell+1)]\\ [2\ell'+1-\rho_{\ell'}]\end{matrix}\right\} \\ -\frac{1}{4}\Lambda_3\nu^4\left(\frac{5}{3}\ell'(\ell'+1)(2\ell'+1)-\left\{\begin{matrix}5\nu^2-1+3\ell'(\ell'+1)-(n^2/\nu^2)\\ [5n^2+1-3\ell(\ell+1)]\end{matrix}\right\}\right) \\ [2\ell'+1-\rho_{\ell'}] \end{bmatrix} \quad (14)$$

is the screened Coulomb normalization constant [9] and

$$N_{p'\ell'} = (2p)^{\ell'}\frac{|\Gamma(\ell'+1+i\nu)|}{\Gamma(2\ell'+2)}e^{\pi\nu/2} \quad (15)$$

is the point Coulomb normalization constant for the continuum state and ν = *a*/*p*.

$$\rho_{\ell'}=\rho_{\ell'-1}+\frac{2\nu^2}{\ell'^2+\nu^2},\quad \rho_0=1-\frac{2\pi\nu}{e^{2\pi\nu}-1} \quad \text{and} \quad \rho_2=\rho_0+\frac{2\nu^2}{1+\nu^2}+\frac{2\nu^2}{4+\nu^2} \quad (16)$$

Thus, the screened continuum radial function is

$$s^{**}_{\ell'}(pr)=s_{\ell'}(pr)+\lambda^2A_2(\ell',pr)+\lambda^3A_3(\ell',pr)+..... \quad (17)$$

where $s_{\ell'}(pr)=M\left(\ell'+1+i\nu,2\ell'+2,2ipr\right)$ (18)

is the usual point Coulomb radial wave function and

$$A_k\left(\ell',pr\right)=\sum_{s=-k}^{k}\alpha_s^k(-i\nu,\ell')M(\ell'+1+i\nu-s,2\ell'+2,2ipr)+ \beta_0^k(-i\nu,\ell')\frac{\partial}{\partial\nu}M(\ell'+1+i\nu,2\ell'+2,2ipr) \quad (19)$$

Here $M(f,g,z)={}_1F_1(f,g,z)/\Gamma(g)$ is the regular confluent hyper-geometric expression and is evaluated from its series expression with argument parameters f, g and z as [11]

$${}_1F_1(f;g;z)=\left\{\sum_{k=0}^{20}\left\{\frac{(f+k-1)!}{(f-1)!}\Big/\frac{(g+k-1)!}{(g-1)!}\right\}\frac{z^k}{k!}\right\}\Big/\Gamma(g) \quad (20)$$

(ii) a. For the continuum state ℓ' = 2, the normalization constant becomes [9]

$$N^{**}_{p'2}=\frac{p^{1/2}(2p)^2}{(2\pi)^{3/2}}\frac{|\Gamma(3+i\nu)|}{\Gamma(6)}e^{\pi\nu/2}\begin{bmatrix}1+0.25\Lambda_2\nu^2\{30-[3\nu^2+16][5-\rho_2]\}\\ -0.25\Lambda_3\nu^4\left(\begin{matrix}50-\{5\nu^2+17-4/\nu^2[15]\}\\ [5-\rho_2]\end{matrix}\right)\end{bmatrix} \quad (21)$$

$$s_2(pr)=M(3+i\nu,6,2ipr) \quad (22)$$

and

$$A_2(2,pr)=\frac{\nu^2V_2}{4a^2}\begin{bmatrix}(21\nu^2+60)M(3+i\nu,6,2ipr)+((3-i\nu)2i\nu(2i\nu-1)-10)\\ M(2+i\nu,6,2ipr)+(0.5i\nu(4-i\nu)(3-i\nu))M(1+i\nu,6,2ipr)+(3+i\nu)\\ [-2i\nu(-2i\nu-1)-10]M(4+i\nu,6,2ipr)-0.5i\nu(4+i\nu)(3+i\nu)M(5+i\nu,6,2ipr)\end{bmatrix} +\frac{4\nu(\nu^2V_2)}{4a^2}\left\{0.5[3\nu^2+6]+5\right\}\frac{\partial}{\partial\nu}M(3+i\nu,6,2ipr) \quad (23)$$

Similarly,

$$A_3(2,pr)=\frac{\nu^4V_3}{4a^3}\begin{bmatrix}-(40\nu^2+52+360/\nu^2)M(3+i\nu,6,2ipr)+(0.5(3-i\nu)(15i\nu)(1-i\nu)+12-120/\nu^2)\\ M(2+i\nu,6,2ipr)+(1.5(1-i\nu)(4-i\nu)(3-i\nu))M(1+i\nu,6,2ipr)-1/6(5-i\nu)(4-i\nu)\\ (3-i\nu)M(i\nu,6,2ipr)+(0.5(3+i\nu)(-15i\nu)(1+i\nu)+12-120/\nu^2)M(4+i\nu,6,2ipr)\\ +1.5(1+i\nu)(4+i\nu)(3+i\nu)M(5+i\nu,6,2ipr)-1/6(5+i\nu)(4+i\nu)(3+i\nu)\\ M(6+i\nu,6,2ipr)\end{bmatrix} +\frac{2\nu(\nu^4V_3)}{4a^3}\left\{-5\nu^2-17+60/\nu^2\right\}\frac{\partial}{\partial\nu}M(3+i\nu,6,2ipr) \quad (24)$$

Thus, the screened continuum radial function for the state ℓ' = 2 becomes

$$s^{**}_2(pr)=M(3+i\nu,6,2ipr)+\lambda^2A_2(2,pr)+\lambda^3A_3(2,pr)+..... \quad (25)$$

and the final form of the continuum wave function is

$$\Re^{**}_{p2}(p'r)=N^{**}_{p'2}r^2e^{-ipr}s^{**}_2(pr) \quad (26)$$

(ii) b. Similarly, for the continuum state ℓ' = 0, the normalization constant becomes [9];

$$N^{**}_{p'0}=\frac{p^{1/2}}{(2\pi)^{3/2}}\frac{|\Gamma(1+i\nu)|}{\Gamma(2)}e^{\pi\nu/2}\begin{bmatrix}1+0.25\Lambda_2\nu^2\{-[3\nu^2+10][1-\rho_0]\}\\-0.25\Lambda_3\nu^4\begin{pmatrix}-\{5\nu^2-1-4/\nu^2[15]\}\\[1-\rho_0]\end{pmatrix}\end{bmatrix} \quad (27)$$

$$s_0(pr)=M(1+i\nu,2,2ipr) \quad (28)$$

and

$$A_2(0,pr)=\frac{\nu^2V_2}{4a^2}\begin{bmatrix}(9\nu^2+20)M(1+i\nu,2,2ipr)+((1-i\nu)2i\nu(2i\nu-1)-10)\\M(i\nu,2,2ipr)+0.5i\nu(2-i\nu)(1-i\nu)M(-1+i\nu,2,2ipr)+(1+i\nu)\\[-2i\nu(-2i\nu-1)-10]M(2+i\nu,2,2ipr)-0.5i\nu(2+i\nu)(1+i\nu)M(3+i\nu,2,2ipr)\end{bmatrix}$$
$$+\frac{4\nu(\nu^2V_3)}{4a^2}\{0.5[3\nu^2]+5\}\frac{\partial}{\partial\nu}M(1+i\nu,2,2ipr) \quad (29)$$

Similarly,

$$A_3(0,pr)=\frac{\nu^4V_3}{4a^3}\begin{bmatrix}-(20\nu^2+2+120/\nu^2)M(1+i\nu,2,2ipr)+(0.5(1-i\nu)(15i\nu)(1-i\nu)-6-120/\nu^2)\\M(i\nu,2,2ipr)+(1.5(1-i\nu)(2-i\nu)(1-i\nu))M(-1+i\nu,2,2ipr)-1/6(3-i\nu)(2-i\nu)(1-i\nu)\\M(-2+i\nu,2,2ipr)+(0.5(1+i\nu)(-15i\nu)(1+i\nu)-6-120/\nu^2)\\M(2+i\nu,2,2ipr)+1.5(1+i\nu)(2+i\nu)(1+i\nu)M(3+i\nu,2,2ipr)-1/6(3+i\nu)(2+i\nu)\\(1+i\nu)M(4+i\nu,2,2ipr)\end{bmatrix}$$
$$+\frac{2\nu(\nu^4V_3)}{4a^3}\{-5\nu^2+1+60/\nu^2\}\frac{\partial}{\partial\nu}M(1+i\nu,2,2ipr) \quad (30)$$

Therefore, the screened continuum radial function for the state ℓ' = 0 becomes

$$s^{**}_0(pr)=M(1+i\nu,2,2ipr)+\lambda^2A_2(0,pr)+\lambda^3A_3(0,pr)+..... \quad (31)$$

and the final form of the continuum wave function for ℓ' = 0

$$\Re^{**}_{p0}(p'r)=N^{**}_{p'0}e^{-ipr}s^{**}_0(pr) \quad (32)$$

The single particle radial integral for bound (L=1) and continuum (ℓ'=2) state reduces as

$$R^{**}_{matrix2}=\int_0^\infty r^3\left[\Re^{**}_2(p'r)\right]^*\left[\Re^{**}_{21}(r)\right]dr \quad (33)$$

Similarly, for L=1 and ℓ' = 0 state

$$R^{**}_{matrix0}=\int_0^\infty r^3\left[\Re^{**}_0(p'r)\right]^*\left[\Re^{**}_{21}(r)\right]dr \quad (34)$$

Thus, for $2p_{3/2}$ state the screened alignment parameter

$$A_2{}^{**}=\frac{\left|R^{**}_{matrix0}\right|^2+\frac{1}{5}\left|R^{**}_{matrix2}\right|^2}{2\left|R^{**}_{matrix0}\right|^2+4\left|R^{**}_{matrix2}\right|^2} \quad (35)$$

To check the authenticity of the present method of calculation of $A_2{}^{**}$, the intermediate steps are compared with our earlier formulation [5] of point Coulomb calculations. A close agreement has been obtained among the values of intermediate steps involved in both the formulations that proved the reliability of these calculations and prompted us to extend our calculations for elements La to U in the energy region threshold to 60 keV. The calculations are performed in mathematica 5.1 and the results are illustrated in Figure 1-5.

5. Results and discussion

The results show that screening has no effect on the shape of plots of $A_2{}^*$ at the lower end of energies but the values are lowered by 4 to 10 % of the earlier values. For the elements $57 \le Z \le 79$ in the energy region 43 to 55 keV like the earlier results [5] on A_2, again the peak structures in $A_2{}^*$ plots appear. For elements $57 \le Z \le 63$ the peak structure is distorted and the gap between two groups of peaks increases, one group shifts comparatively to lower energy and other shifts to higher energy side (Figure 1). For the elements $64 \le Z \le 73$, the peak shifting is less but the peak becomes more prominent as compared to the case of without screening (Figure 2). The peak structure in Figure 3 for W shows the pattern similar to shifting of lower group of peaks in case of La and the trend remains the same up to Pt. For Au slight peak structure in $A_2{}^*$ appears at the high energies that was almost absent for A_2 in the same energy region (Figure 4).

Similar $A_2{}^*$ peaks, though low in intensity, appear for elements Z=81 to 83. All this confirms that peak structures have shifted to lower energy side. For elements Z>83 there is smooth fall in $A_2{}^*$ with energy (Figure 5). The peak structures may be due to some disturbance of the point Coulomb potential with the starting of the K shell ionization and the explanation [5] still holds with screening effects though there is shift in energy.

Alignment parameter $A_2{}^{**}$ takes maximum value (~0.5) in the regions starting from L3 threshold energy to about 30 to 45 keV for all the elements. The range shifts to higher energy side for increasing Z's. For the elements with Z varying from 57 to 70 a decrease in the alignment value exists at ~30 keV (Figure 1-4).This downfall in the alignment also increases with Z's and attains its least value ~ 0.05 for the most of the elements. Moreover, this down fall is in the form of peak structure in the energy region 40 to 50 keV. The alignment remains almost constant (~0.5) for all the high Z elements in the range 81 to 92 with a very small variation at the third decimal place throughout whole energy range (Figure 5). The alignment parameter values being > 0.1 at energies < 20 keV are certainly higher than 5 to 8% uncertainties quoted in experimental results. The presence of energy pockets where the alignment is comparatively prominent requires further exploration either with the precise measurements of low intensity L x-rays (L_ℓ and $L_{\alpha 2}$) or by modifications of theoretical calculations. In Figures 1-5, $A_2{}^{**}$ looks just as reflection or complement of variations in A_2 and $A_2{}^*$ values. Therefore, the explanation for the peak structure [5] may still be appreciable for the screening effect derived through analytical perturbation theory.

References

[1]. Flügge, S.; Mehlhorn, W.; Schmidt, V. *Phys. Rev. Lett.* **1972**, *29*, 7-9.
[2]. Berezhko, E. G.; Kabachnik, N. M.; Rostovsky, V. S. *J. Phys. B.* **1978**, *11*, 1749-1758.
[3]. Kleiman, U.; Lohmann, B. *J. Elect. Spectro. Rel. Phen.* **2003,** *131*, 29-50.
[4]. Sharma, A.; Mittal, R. N. *Instr. Meth. Phys. Res. A.* **2010**, *619*, 55-58.
[5]. Sharma, A.; Singh, M.; Mittal, R. *Pramana* **2006**, *66*, 1111-1118.
[6]. Slater, J. C. *Phys. Rev.* **1930**, *36,* 57-65.
[7]. McEnnan, J.; Kissel, L.; Pratt, R. H. *Phys. Rev. A* **1976**, *13*, 532-558.
[8]. Hall, H. *Rev. Mod. Phys.* **1936**, *8*, 358-359.
[9]. Sharma, A.; Mittal, R. Vacancy alignment in atomic inner shells, Lambert Academic Publishing, 2010.
[10]. Oh, S. D.; McEnnan, J.; Pratt, R. H. *Phys. Rev. A.* **1976**, *14*, 1428-1436.
[11]. Wolfram, S. The Mathematica, Cambridge University Press, 1996.